Formation of Microporous Polymeric Materials By Microemulsion Polymerization of Methyl Methacrylate and 2-Hydroxyethyl Methacrylate

T. H. CHIENG,[1] L. M. GAN,[1] C. H. CHEW,[1] S. C. NG,*[2] and K. L. PEY[3]

[1]Department of Chemistry, [2]Department of Physics, and [3]Institute of Microelectronics, National University of Singapore, Republic of Singapore

SYNOPSIS

The investigated microemulsion system consisted of methyl methacrylate, 2-hydroxyethyl methacrylate and water using sodium dodecyl sulphate as surfactant. Ethylene glycol dimethacrylate acting as a cross-linker was also incorporated to enhance the mechanical strengths of the microporous polymeric materials. The polymerization was carried out at room temperature using a reactive redox initiator comprising ammonium persulphate and *N,N,N',N'*-tetramethylethylene diamine. The conductivities of the microemulsion samples were monitored during the course of polymerization. The conductivities for a bicontinuous microemulsion before and after polymerization were found to be very similar. In addition, the transformation of microstructures was also examined using a transmission as well as a field emission scanning electron microscope. It is evidenced from the micrographs that microporous polymeric materials prepared from bicontinuous microemulsion polymerization are attributed to numerous coagulations of spherical particles. A possible mechanism for the microstructural transformation is discussed based on the information of conductivity measurements and electron micrographs. © 1996 John Wiley & Sons, Inc.

INTRODUCTION

Since the introduction of microemulsion by Schulman,[1] many studies on the kinetics and mechanisms of monomer polymerization in oil-in-water (O/W) and water-in-oil (W/O) microemulsions have been reported.[2-6] Microemulsions exhibiting microstructures are thermodynamically stable.[7-9] The various microstructures are dependent on the composition of the system. It has been suggested[10] that electrical conductivity measurement could provide, along with other techniques, valuable information about the structure and phase behavior of microemulsions. In fact it has already been employed by many workers[11,12] to study the transformation of W/O to O/W microemulsions through the bicontinuous state.[13,14]

Recently, much interest has been focussed on the study of the formation of porous polymeric materials by polymerizing monomer(s)-containing bicontinuous microemulsions.[15-20] To our knowledge, the understanding about the formation of the microstructures in porous polymeric materials from microemulsion polymerization is still very limited. Stoffer and Bone[21] observed globular structure in the polymeric solids formed from microemulsion polymerization, but no explanation was given to their formation. Our recent studies[22,23] also showed the formation of globular microstructures of polymeric materials from microemulsion polymerization of methyl methacrylate and 2-hydroxyethyl methacrylate using a nonpolymerizable surfactant of sodium dodecyl sulphate (SDS) or *n*-dodecyltrimethyl ammonium bromide. This paper is a follow-up study of the previous work[22] on microporous polymeric materials, providing additional information about the formation of the microstructures.

* To whom correspondence should be addressed.

Journal of Applied Polymer Science, Vol. 60, 1561-1568 (1996)
 CCC 0021-8995/96/101561-08

EXPERIMENTAL

Materials

Methyl methacrylate (MMA) from BDH, 2-hydroxyethyl methacrylate (HEMA) and ethylene glycol dimethacrylate (EGDMA) from Merck were vacuum distilled to remove impurities and inhibitors before use. The redox initiator consisting of *N,N,N',N'*-tetramethylethylene diamine (TMEDA) and ammonium persulphate (APS) of purity greater than 99 and 98%, respectively, was used as received from Aldrich. SDS of purity greater than 99% was used as received from TCI, Japan. Millipore water of electrical conductivity ca. 1.0 μS cm^{-1} was used.

Polymerization

Details of the microemulsion preparation and characterization were described in the previous study.[22] A redox initiating system (APS/TMEDA)[24] was used for the polymerization. An air-tight glass tube with carbon electrodes and a rubber septum inserted at the open end was purged with nitrogen gas via needles before the microemulsion sample was introduced into the tube with a syringe. The amount of initiator used was always 13.1 mmol (0.3 wt %), based on the total weight of the aqueous phase for each system with the composition shown in Table I. The polymerization was carried out for 2 h at 20°C in an air conditioned room. The conductivity was monitored during the polymerization. In addition, polymer conversions were also monitored for microemulsion samples WO12 and BC48. A series of ampules containing each sample were polymerized for different durations of time. At the end of each duration time, the sample was washed in a large quantity of methanol and then was leached in hot water at 50°C for a week to remove all the unpolymerized monomers and surfactant. The final polymer conversion, based on the total amount of monomers added in the precursor systems, was calculated.

Conductivity Measurement

The conductance of each microemulsion sample σ was monitored during the course of polymerization using a 2340 LCZ meter (NF Electronic Instruments) at 20 ± 0.5°C. The frequency was set at 1 kHz. Two inert carbon plates of surface area A of 0.375 cm^2 each were used as the electrodes. The conductivity of the polymerizing microemulsion sample κ was calculated according to the equation

Table I Microemulsion Compositions for Polymerization*

Microemulsion System†	MMA (wt %)	HEMA (wt %)	SDS (wt %)	Water (wt %)
WO12	51	34	3	12
BC48	24	16	12	48
OW76	3	2	19	76

* The weight ratio of MMA : HEMA was fixed at 3 : 2, and SDS to water at 1 : 4. EGDMA added was 4 wt % based on the total weight of MMA and HEMA, and redox initiator APS/TMEDA was 0.3 wt % based on the aqueous phase.

† The symbols WO, BC, and OW represent water-in-oil, bicontinuous, and oil-in-water microemulsions respectively. The numbers after each symbol denote the water content for each system.

$$\kappa = A\sigma/d$$

where d is the distance between the two carbon plates.

Morphology Observation

The polymerized samples before the onset of gelation were examined by a JEOL JEM-100CX transmission electron microscope (TEM). One drop of the latex was deposited onto a copper grid coated with a thin layer of Formvar. After being air dried, the sample on the copper grid was stained by dipping it in a 0.5 wt % phosphotungstic acid (PTA) solution. The sample was then air dried again before it was examined under the microscope. The gelled samples were examined by a field emission scanning electron microscope (FESEM, Hitachi S-4100). In this case, samples were first frozen in liquid nitrogen and then were fractured mechanically. The fractured samples were vacuum dried for 24 h at room temperature before being coated with gold using a JEOL ion-sputter JFC-1100 coating machine.

RESULTS

The phase behavior of the microemulsion system consisting of MMA/HEMA/SDS/water with ethylene glycol dimethacrylate as a cross-linking agent was previously studied by us.[22] The phase diagram is reproduced in Figure 1 to provide information on the microstructures related to the various types of microemulsions. The microemulsion compositions (Table I) chosen for polymerization study lie on the line L drawn on the phase diagram. Our earlier investigation on the system shows that the single-

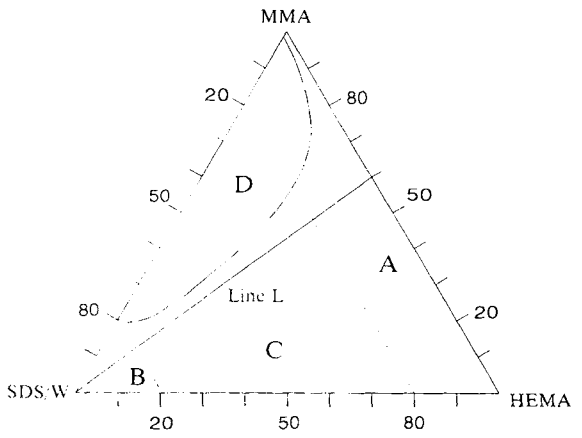

Figure 1 The phase diagram for the system MMA/HEMA/SDS/water (W), and ethylene glycol dimethacrylate (EGDMA) at 30°C. EGDMA added was 4.0 wt % based on the total weight of MMA and HEMA. SDS used was 20 wt % in water. Domains: A, W/O microemulsion; B, O/W microemulsion; C, bicontinuous microemulsion; D, two-phase region.

phase microemulsion comprises three types of microstructures dependent on the water content of the system. They are W/O droplet structure at low water content (<20 wt %), O/W droplet structure at high water content (>70 wt %), and bicontinuous structure at intermediate water content.

The polymerization was carried out using a reactive redox initiator, APS/TMEDA, which has an advantage over the thermal decomposed initiator because polymerization can be done at room temperature, thus alleviating the occurence of phase separation. Microemulsion compositions listed in Table I were chosen to investigate the conductivity behavior, polymer conversion, and change of microstructures of the microemulsion samples during the course of polymerization. The compositions (in wt %) chosen were based on the phase behavior studies that show different types of microstructures, i.e., sample WO12 was a W/O microemulsion, sample BC48 a bicontinuous microemulsion, and sample OW76 an O/W microemulsion. For samples WO12 and BC48, the gelation started within 10 min of polymerization.

The conductivity behavior of sample WO12 and its corresponding polymer conversion during the course of polymerization are shown in Figure 2. The conductivity decreased gradually within the first 50 min of polymerization up to about 40% polymer conversion. It then sharply decreased on further polymerization up to about 70 min or 75% conversion. Thereafter, the changes of conductivity and polymer conversion became slower again. Polymer conversion as a function of polymerization time behaved in a reverse manner. The decrease of conductivity before and after polymerization of the sample was about four-fold. The morphology of the polymerized sample WO12 at different polymerization times and their respective polymer conversions are shown in Figure 3(a)-(c). The pores sizes of the sample after 30 min of polymerization ranged from ca. 0.5 to 15 μm, and they decreased to ca. 0.5–2 and 0.1–0.3 μm after 70 and 120 min of polymerization, respectively.

The variation of the conductivity for sample BC48 during polymerization as depicted in Figure 4 was very different from that of sample WO12. It showed a sharp increase in conductivity to a maximum at about 60% polymer conversion within 30 min of polymerization. The conductivity then decreased sharply from about 60 to 90% conversion. The initial first minute of polymerization produced spherical polymer particles ca. 80–100 nm in diameter, as can be clearly seen from the TEM micrograph [Fig. 5(a)]. These primary polymer particles merged with each other and grew to micron size after 5 min of polymerization as illustrated by the TEM micrograph [Fig. 5(b)].

On further polymerization, the whole microemulsion system transformed into a turbid soft gel and finally an opaque solid. After 30 min of polymerization with conversion at ca. 60%, the morphology of the polymeric material as revealed by FESEM micrographs of Figure 6 shows the existence of smaller globular structures coagulated with the larger aggregates. Figure 6(a) and (b) show the polymeric surface that was in contact with the glass wall and the fractured surface in the glass tube, re-

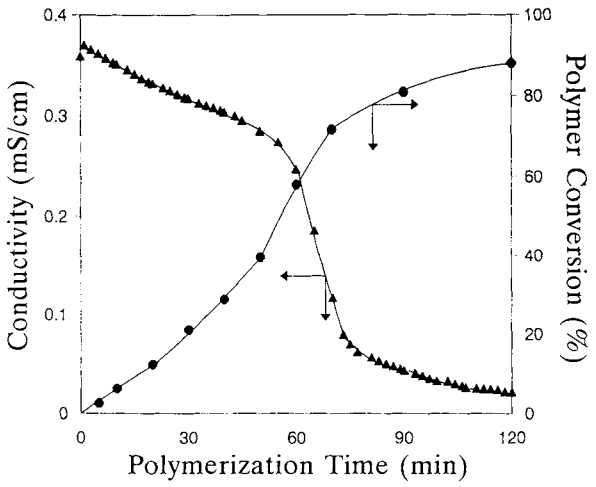

Figure 2 The conductivity curve for sample WO12 and its corresponding polymer conversion as a function of polymerization time.

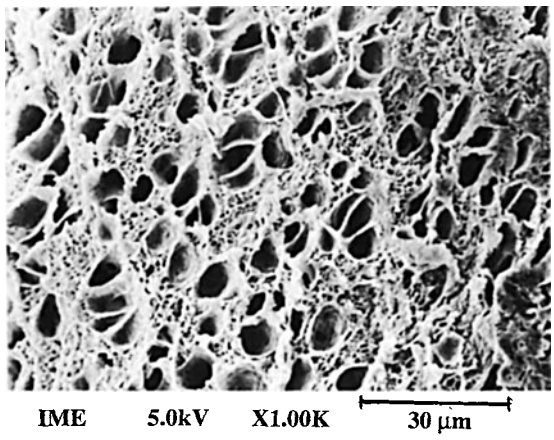

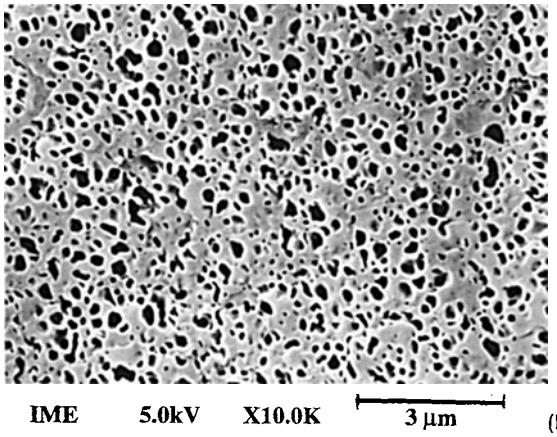

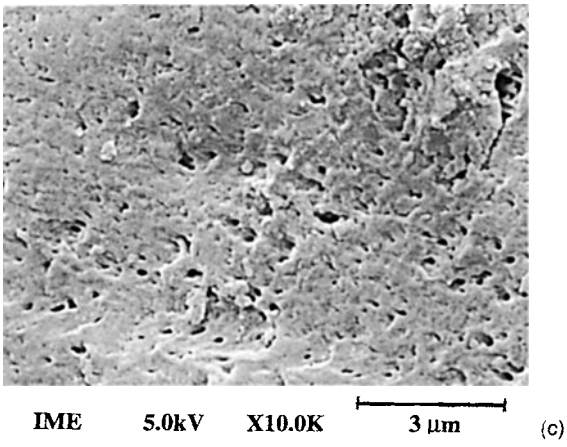

Figure 3 FESEM micrographs of the fractured polymer sample WO12 at different polymerization times and the corresponding polymer conversions. (a) 30 min (21%). (b) 70 min (71.7%). (c) 120 min (89%).

spectively. These smaller globular structures were not observed after 60 min of polymerization, as revealed by FESEM micrographs (Fig. 7). Figure 7(a) and (c) show the polymeric surfaces that were in contact with the glass wall and were exposed to the nitrogen atmosphere in the glass tube, respectively, and Figure 7(b) shows the fractured surface of the same polymer sample. Interconnected globular structures can be clearly discerned from FESEM micrographs. Moreover, polymer threads joining the globular structures can also be seen from Figure 7(a) and (c). As a result of these interconnected globular structures, voids or random porous structures were formed. The pores of dimension ca. 0.5–1.5 μm can clearly be seen from Figure 7(c).

The conductivity of the polymerized samples (after 2 h of polymerization) as a function of the water content of the precursor microemulsions is shown in Figure 8. They remained low for those polymers prepared from the precursor microemulsion exhibiting W/O droplet structures. For microemulsion samples containing 20–40 wt % water, the conductivity of the systems before and after polymerization were seen to increase in parallel. At higher water contents (>40 wt %), the conductivity for the precursor microemulsions continued to increase, whereas the conductivity for the corresponding polymerized samples remained about the same. This resulted in the increasing disparity in conductivity between microemulsion samples before and after polymerization when the water content in the systems were further increased.

Although this work emphasizes the study of formation of microporous polymeric materials from W/

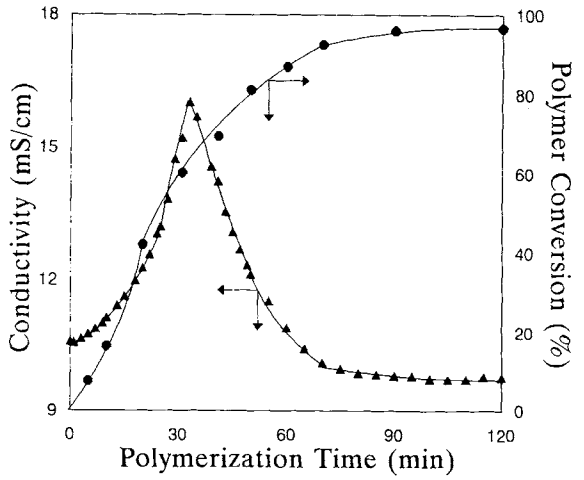

Figure 4 The conductivity curve for sample BC48 and its corresponding polymer conversion as a function of polymerization time.

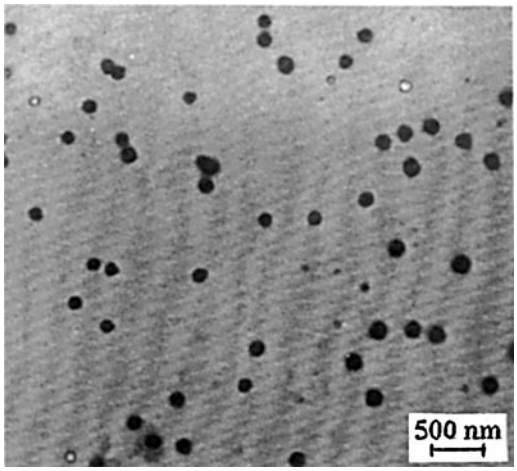

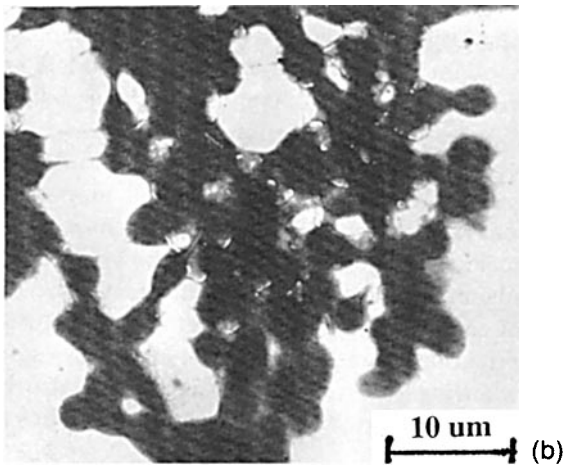

Figure 5 TEM micrographs of the sample BC48 before gelation at different polymerization times and the corresponding polymer conversions. (a) 1 min (1.8%). (b) 5 min (7.5%).

O and bicontinuous microemulsions, results of O/W microemulsion polymerization are also included here for comparisons. The variation in conductivity during polymerization for sample OW76 as depicted in Figure 9 is quite striking. Sample OW76 was an O/W microemulsion and it formed polymer particles after polymerization as shown by the TEM micrograph in Figure 10. The polymerization proceeded with increasing viscosity and ended with a clear viscous fluid. It is noted that the polymer particles were irregular in shape, resulting from apparent mergers of the spherical particles. This may be due to the surface characteristics of the copolymer particles of MMA and HEMA.

DISCUSSION

The conductivity of the systems was mainly due to the presence of the ionic species of SDS in the microemulsions. The continuous decrease in the conductivity of the polymerized W/O microemulsion (sample WO12) was due to the continuous reduction in the mobility of the water droplets upon polymerization. The reason is that these water droplets were progressively isolated from each other when the monomers–continuous phase was gradually converted to the solid polymer during polymerization. The larger pores or voids, almost round in shape as

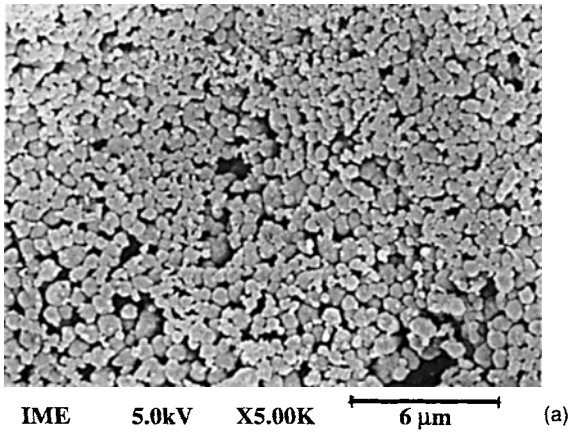

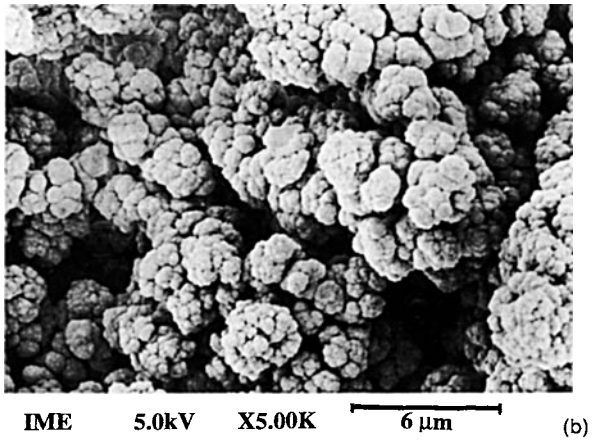

Figure 6 Micrographs of FESEM for sample BC48 at 30 min of polymerization with 60.2% polymer conversion. (a) Polymer surface in contact with the glass wall of the glass tube. (b) Fractured surface of the polymer sample.

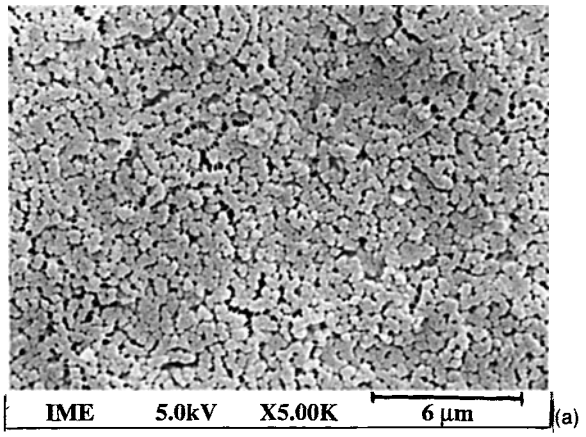

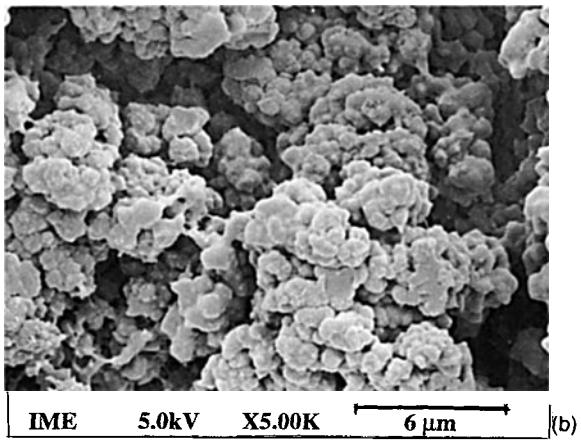

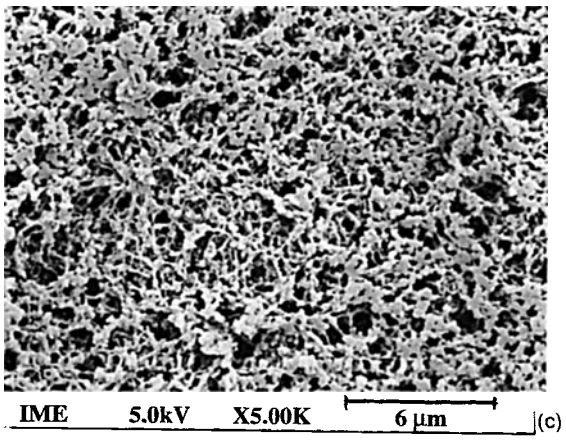

Figure 7 Micrographs of FESEM for sample BC48 at 60 min of polymerization with 87% polymer conversion. (a) Polymer surface in contact with the glass wall of the glass tube. (b) Fractured surface of the polymer sample. (c) Polymer surface facing the nitrogen atmosphere during polymerization.

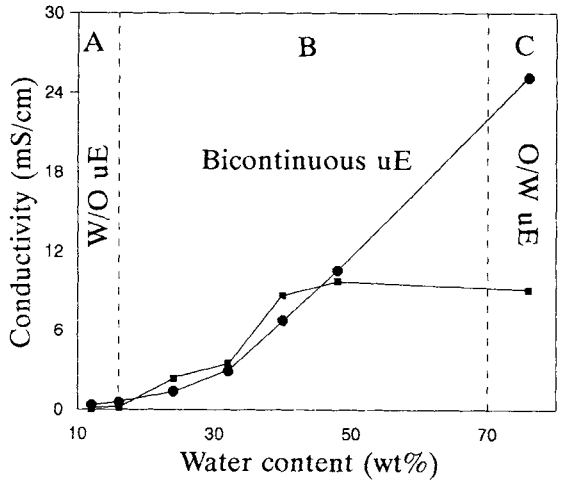

Figure 8 The conductivity curves of the precursor microemulsions (—●—) and its respective polymerized samples (—■—) as a function of the water content in the system.

seen from Figure 3(a) and (b), are believed to be the spaces originally occupied by both water domains and unpolymerized monomers, which were left behind after their removal from the polymer matrix. At higher polymer conversion, the much reduced pores or voids sizes (0.1–0.3 μm) were mainly due to the removal of water, as almost all monomers were converted to polymers. However, these pores still appear too large compared with the original microemulsion droplet and thus indicate the occurrence of coalescence between water droplets during polymerization. Some deformation of the pores occurring during the fracturing process can also be seen in the micrographs. The formation of pores of

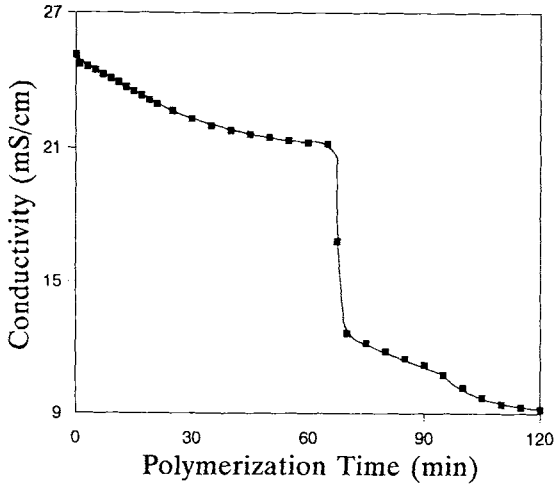

Figure 9 The conductivity curve for sample OW76 as a function of polymerization time.

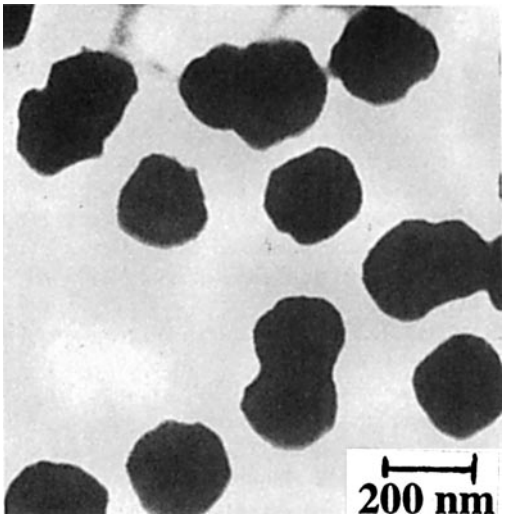

Figure 10 TEM micrograph of polymer particles for sample OW76 after 2 h of polymerization.

spherical shape also indicates that the precursor microemulsion consisted of spherical W/O droplet structures. These pores, which were observed in our previous study,[22] are of the closed-cell structure and are not interconnected. It is known that the closed-cell-type structures are formed form W/O microemulsions. The information derived from the conductivity measurement provides additional evidence that the microstructure of the W/O microemulsion changed from initial W/O droplets to closed-cell structure after polymerization.

The decreasing conductivity observed for the O/W microemulsion polymerization (sample OW76) was attributed to the continuous increase in the viscosity of the system, resulting in reducing the movement of ionic species. The increase in the viscosity of the polymerized system was due to the production of much larger polymer particles (ca. 150–200 nm) arising from the mergers of particles as shown in Figure 8.

The polymerization of monomers in bicontinuous microemulsions characterized by low interfacial tension ($\sim 10^{-3}$ dyn cm^{-1}) initially produced spherical polymer particles. This behavior has also been observed in the other polymerization systems of isotropic bicontinuous microemulsions.[25,26] The bicontinuous structure ruptured as soon as the polymerization started because of the formation of very large macromolecules in the aqueous and/or oil domains, which increased the interfacial tension leading to the formation of spherical polymer particles. These particles seemed to grow rapidly, and they coagulated with each other to form an interconnected aggregates. The continuous increase in polymer particle size also explains why the initial clear microemulsion changed into a final opaque solid. The newly formed smaller particles of faster diffusion collided with the larger matured polymer particles and anchored to them via the strong attractive hydrophobic interactions as evidenced from Figure 6. These smaller particles might then swell by recruiting monomers from oil continuous phase and grew into bigger particles. Because the polymer particles were very close to each other, the process of coagulation between them was bound to happen via the strong attractive hydrophobic interactions. As polymer particles grew, new surface areas were created, causing the distance between the stabilizing moieties to increase and thus rendering heterocoagulation. Besides, an explosive increase in the number of polymer particles would require a fast supply of surfactant for stabilization. The rate of redistribution of surfactant for particle stabilization, however, might be retarded by the ever increasing viscosity of the system upon polymerization. Hence, the poorly protected surfaces of the copolymer particles would continuously coagulate upon collisions between the highly concentrated particles. The voids (pores) are believed to be the water-filled spaces generated between the incompletely coalesced spherical aggregates, as was observed in our previous studies.[22,23] In addition, the presence of aggregated structures has also been reported for polymer composites by an emulsion method.[27,28]

The similarity in high conductivities between the precursor bicontinuous microemulsions (Fig. 4) and the polymerized sample indicates that the water domains in the polymer matrix are still well interconnected. However, it is intriguing to note that the conductivity of the microemulsion sharply increased to a maximum (16 mS cm^{-1}) at about 60% polymer conversion before it reduced equally sharply to a slightly lower value (9.5 mS cm^{-1}) than its original one (10.5 mS cm^{-1}). The sharp increase in conductivity during the early stage of polymerization may be due to the continuous coagulation of spherical polymer particles leading to the desorption of surfactant molecules into the aqueous medium and also the occurrence of phase separation, which caused the coalesence of water domains. These coalesced water domains of sizes much larger than the typical channel width of bicontinuous structure (60–80 nm)[29,30] allowed easy transport of ionic species and thus increased the conductivity. This explanation is also consistent with the morphology observation showing pores of dimension in the submicron and micron range. Thereafter, the increase in the viscosity of the polymer matrix might markedly retard

the mobility of ionic species in the interfacial regions, leading to the sharp decrease in conductivity.

CONCLUSIONS

The different microstructures of the precursor microemulsions give rise to different conductive behaviors during the course of polymerization. The monitoring of the conductivity for a bicontinuous microemulsion can be carried out until it forms a polymer solid. The conductivities of a precursor bicontinuous microemulsion and its polymerized sample are found to be very similar, indicating the presence of bicontinuous structures. However, the microstructures of the precursor bicontinuous microemulsion may not be directly related to the interconnected microporous structures in the polymer matrix. The latter is deemed to be the water-filled voids generated from the numerous coagulations of spherical particles as evidenced from FESEM micrographs.

We are grateful to Mdm. Loy of Zoology Department, National University of Singapore, for her assistance in taking TEM micrographs. Authors also thank to National University of Singapore for the financial support under grants 890638 and 930630.

REFERENCES

1. J. H. Schulman, *Nature,* **152,** 102 (1943).
2. V. H. Perez-Luna, J. E. Puig, V. M. Castano, B. E. Rodriguez, A. K. Murthy, and E. W. Kaler, *Langmuir,* **6,** 1040 (1990).
3. M. Antonietti, W. Bremser, D. Muschenborh, C. Rosenauer, B. Schupp, and M. Schmidt, *Macromolecules,* **24,** 6636 (1991).
4. L. M. Guo, E. D. Sudol, J. W. Vanderfoff, and M. S. El-Aasser, *J. Polym. Sci., Polym. Chem. Ed.,* **30,** 691 (1992).
5. F. Candau, in *Polymerization in Organized Media,* M. Paleos, Ed., Gordon and Breach Science Publishers, Philadelphia, 1992, Chapt. 4, p. 215.
6. L. M. Gan, C. H. Chew, K. C. Lee, and S. C. Ng, *Polymer,* **34,** 3064 (1994).
7. P. A. Winsor, *Trans. Faraday Soc.,* **44,** 376 (1948).
8. B. Lagourette, J. Peyrelasse, C. Boned, and M. Clausse, *Nature,* **281,** 60 (1979).
9. S. E. Friberg and P. Bothorel, Eds., *Microemulsions : Structure and Dynamics,* CRC Press Inc., New York, 1986.
10. M. Clausse, J. Heil, J. Peyrelasse, and C. Boned, *J. Colloid Interface Sci.,* **87,** 584 (1982).
11. M. Clausse, A. Zradba, and L. Nicholas-Morgantini, in *Microemulsion Systems,* H. L. Rosano, and M. Clausse, Eds., Marcel Dekker Inc., New York, 1987, p. 387.
12. S. J. Chen, D. F. Evans, and B. W. Ninham, *J. Phys. Chem.,* **264,** 896 (1986).
13. L. E. Sciven, *Nature,* **263,** 123 (1974).
14. P. Pieruschka and S. Marcelja, *Langmuir,* **10,** 345 (1994).
15. S. Qutubuddin, E. Haque, W. J. Benton, and E. J. Fendler, in *Polymer Association Structures : Microemulsion and Liquid Crystals,* ACS Symposium Series 384, M. A. El-Nokaly, Ed., 1989, p. 64.
16. M. Sasthav and H. M. Cheung, *Langmuir,* **7,** 1378 (1991).
17. W. R. Palani Raj, M. Sasthav, and H. M. Cheung, *Langmuir,* **7,** 2586 (1992).
18. W. R. Palani Raj, M. Sasthav, and H. M. Cheung, *Langmuir,* **8,** 1931 (1992).
19. W. R. Palani Raj, M. Sasthav, and H. M. Cheung, *J. Appl. Polym. Sci.,* **47,** 499 (1993).
20. L. M. Gan, T. H. Chieng, C. H. Chew, and S. C. Ng, *Langmuir,* **10,** 4022 (1994).
21. J. O. Stoffer and T. Bone, *J. Dispersion Sci. Technol.,* **1,** 393 (1980).
22. T. H. Chieng, L. M. Gan, C. H. Chew, and S. C. Ng, *Polymer,* **36,** 1941 (1995).
23. T. H. Chieng, L. M. Gan, C. H. Chew, L. Lee, S. C. Ng, K. L. Pey, and D. Grant, *Langmuir,* **11,** 3321 (1995).
24. X. Q. Guo, K. Y. Qiu, and X. D. Feng, *Makromol. Chem.,* **191,** 577 (1990).
25. F. Candau, Z. Zekhnini, and J. P. Durand, *J. Colloid Interface Sci.,* **114,** 398 (1986).
26. C. Holtzscherer and F. Candau, *J. Colloid Interface Sci.,* **125,** 97 (1988).
27. E. Rukenstein and F. Sun, *J. Appl. Polym. Sci.,* **46,** 1271 (1992).
28. E. Rukenstein and H. Li, *Polymer,* **35,** 4343 (1994).
29. J. F. Bodet, J. R. Bellare, H. T. Davis, L. E. Sciven, and W. G. Miller, *J. Phys. Chem.,* **92,** 1898 (1988).
30. W. Jahn and R. Strey, *J. Phys. Chem.,* **92,** 2294 (1988).

Received April 11, 1995
Accepted July 29, 1995